Journal of
Ceramic Science
and Technology

J. Ceram. Sci. Tech., **04** [01] 19-24 (2013)
DOI: 10.4416/JCST2012-00034a
available online at: http://www.ceramic-science.com

Hybrid Laser Ablation of Al_2O_3 Applying Simultaneous Argon Plasma Treatment at Atmospheric Pressure

C. Gerhard*[1, 2], S. Roux[3], F. Peters[4], S. Brückner[1, 2], S. Wieneke[4], W. Viöl[2, 4]

[1]Clausthal University of Technology, Institute of Energy Research and Physical Technologies, Leibnizstrasse 4, 38678 Clausthal-Zellerfeld, Germany
[2]Fraunhofer Institute for Surface Engineering and Thin Films, Application Center for Plasma and Photonic, Von-Ossietzky-Strasse 99, 37085 Göttingen, Germany
[3]Institut d'Optique Graduate School, RD 128 - Campus Polytechnique, 2, Avenue Augustin Fresnel, 91127 Palaiseau Cedex, France
[4]University of Applied Sciences and Arts, Laboratory of Laser and Plasma Technologies, Von-Ossietzky-Strasse 99, 37085 Göttingen, Germany
received September 24, 2012; received in revised form November 16, 2012; accepted January 9, 2013

Abstract

In this work, we present a hybrid laser-plasma ablation technique for material processing of ceramics. Atmospheric pressure argon plasma treatment as well as laser ablation and hybrid laser-plasma ablation experiments were performed on aluminium oxide in order to investigate the impact of the assisting plasma in terms of material removal efficiency and energy-related aspects. It was shown that by means of pure plasma treatment, surface roughness was decreased, resulting in an increase in surface energy and polarity, respectively. Further, by simultaneously applying a plasma beam at atmospheric pressure to a laser ablation process, the ablated area on the aluminium oxide surface was increased while the form error was partially reduced. Spectroscopic measurements of the ablation plume for pure laser ablation and laser-plasma ablation were performed. It was shown that with the assisting plasma, characteristic spectral lines of aluminium were intensified. Further, other Al-spectral lines that were not observed in the case of pure laser ablation were detected, corresponding to higher material removal owing to energetic synergies of both the laser ablation process and the assisting plasma.

Keywords: Aluminium oxide, laser ablation, atmospheric pressure plasma, hybrid laser-plasma ablation

I. Introduction

Thanks to its advantageous electrical and mechanical properties, aluminium oxide (Al_2O_3) is one of the most important ceramics for a number of different applications. Besides high electrical insulation and high dielectric strength, Al_2O_3 features high-temperature stability as well as good tribological characteristics such as low friction and low abrasion. For instance, it is used as an insulator in electric circuits, a dielectric for capacitors or bearing material for measuring instruments or the running surfaces of prostheses. In some micro-electro-mechanical systems (MEMS), circuit boards, including for use in a heat sink function, are made of aluminium oxide. This material is also used as a dielectric base layer or gate dielectric for thin film transducers [1]. In this context, the surface quality of such layers directly impacts the device performance. One possibility for realizing high-quality Al_2O_3 film surfaces is lapping and polishing [2], which is also a technique applied for structuring defined throat heights [3]. However, such techniques are limited with regard to the finishing of complex-shaped workpieces. Against these backgrounds, both smoothing and laser micro-machining of this widely used ceramic material are of great interest.

Generally, a number of different laser sources such as CO_2-, Nd:YAG- and excimer lasers are suitable for cutting ceramics, where the use of short pulses for ablation allows a reduction or mitigation of disturbing thermal effects [4]. With application of near-infrared (NIR) lasers with pulse durations in the femtosecond range, high edge quality and minimization of material melting can be achieved [5,6]. Further, with the introduction of a blower and vent system to femtosecond laser micro-drilling of Al_2O_3, high hole qualities result in the case of trepanning [7]. Laser drilling of aluminium oxide has also been performed with the use of Nd:YAG lasers with pulse durations in the picosecond and nanosecond range [8,9]. However, several process parameters such as laser wavelength, pulse duration, laser intensity and the composition of the ambient atmosphere have a strong influence on the ablation results [10]. In the case of XeCl excimer laser ablation of Al_2O_3, it was shown that the process efficiency can be improved by means of several enhancements such as increasing the material temperature or applying a water film

* Corresponding author: gerhard@hawk-hhg.de

to the ceramic surface [11]. In this work, we present a hybrid laser ablation method for ablating Al_2O_3. This technique is based on a combination of ultraviolet laser irradiation with pulse durations in the range of some nanoseconds with simultaneous application of an argon plasma beam at atmospheric pressure.

II. Experimental Setup and Procedure

Atmospheric pressure plasma treatment and hybrid laser-plasma ablation experiments were performed on ceramic samples made of sintered rhombohedral (trigonal) α-Al_2O_3 from Friatec Frialit-Degussit (Mannheim, Germany) with a purity of > 99.5 wt%. Here, a rotation-symmetric cone-shaped plasma nozzle was used [12]. Based on a dielectric barrier discharge (DBD), this plasma source provides a low-temperature plasma in non-thermal equilibrium [13]. By the geometry of the gas channel between the internal high-voltage (HV) copper electrode and the surrounding plastic housing, the formed plasma is stabilized to a fine plasma filament with a diameter of approx. 200 µm between the HV-electrode and the exterior ground (GND) electrode. The electrodes are separated dielectrically by the ceramic sample. During the experiments, argon (Ar) 4.6 from Linde (Pullach, Germany) was used as working gas; the gas flow rate was approx. four standard litres per minute (slm). The hollow-core geometry of the HV-electrode allows coaxial access to the plasma filament. This access was used to guide the processing laser beam along the formed plasma as shown in Fig. 1.

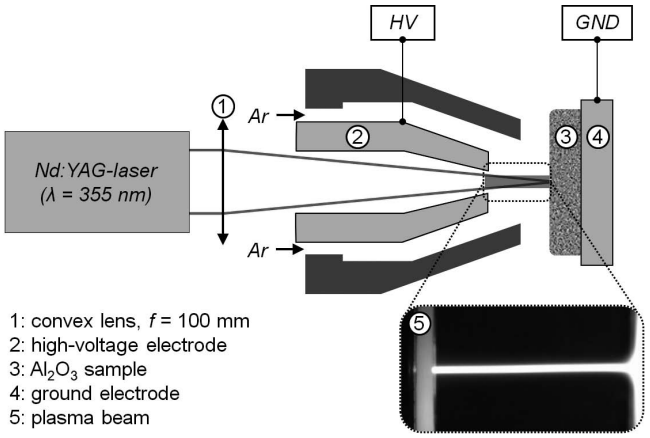

Fig. 1: Experimental setup for atmospheric pressure plasma-assisted laser ablation of Al_2O_3.

For each HV-pulse train, the plasma energy E_{plasma} was 0.17 mJ. Owing to the applied pulse repetition rate f_{rep} of 7 kHz, the averaged power P_{av} thus amounted to 1.19 W. The processing laser beam was provided by a third-harmonic Nd:YAG-laser Powerlite 9010 from Continuum (Santa Clara, USA) with a wavelength λ of 355 nm. The laser was operated in single pulse mode with a pulse duration Δt of 8 ns and at three different energies per pulse E_{pulse} of 7.7, 35.7 and 95.9 mJ, respectively. A plano-convex lens with a focal length f of 100 mm was used to focus the laser beam onto the sample surface. Subsequently, 5 – 40 laser shots were applied to the sample surface.

In order to evaluate the influence of the assisting plasma, both laser-ablated and laser-plasma-ablated samples were investigated with a scanning electron microscope (SEM) PSEM eXpress from Aspex (Delmont, USA). Further, the resulting ablation plumes during the ablation experiments were analysed with the aid of optical emission spectroscopy as shown in Fig. 2.

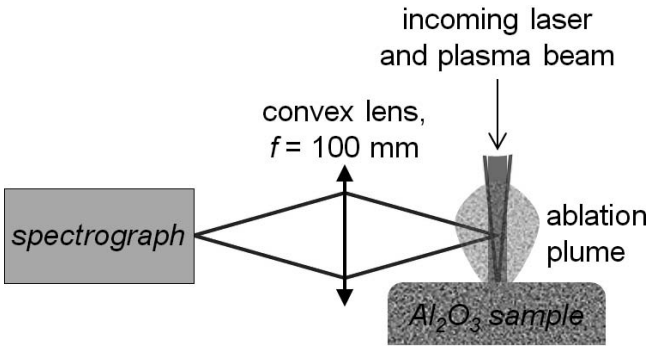

Fig. 2: Setup for spectroscopic measurement of the ablation plume.

Such spectroscopic measurement allows definite determination of the composition of the ablated material [14]. A SpectraPro-300i spectrograph from the Acton Research Corporation (Acton, USA) was used to perform measurement when applying the pure plasma filament, the pure laser beam and the combination of both onto the sample surface.

Further, to investigate the influence of the pure plasma filament on the sample surface, plasma treatment was performed for 60 s. Subsequently, the plasma-induced change of the arithmetic mean surface roughness *Ra* and the roughness root mean square *RMS* were determined with an atomic force microscope (AFM) easyScan 2 AFM from Nanosurf (Liestal, Switzerland). In addition, the surface energy γ and the associated polarity *P*, which is given by the ratio of both the polar fraction and the total amount of the surface energy, of untreated and plasma-treated Al_2O_3 were detected with the aid of a contact angle measurement system G10 from Krüss (Hamburg, Germany).

III. Results and Discussion

(1) Pure plasma treatment

The surface roughness of an area measuring $50 \times 50\ \mu m^2$ was determined before and after 60-second plasma treatment. Based on the measured values, the specific percentual change was calculated. As shown in Table 1, a plasma-induced surface smoothing of the sample surface results. Such a decrease in surface roughness using the above-described setup was already observed in previous work in which different optical glasses were investigated [15]. It can be assumed that the plasma discharge causes high electric field strengths at roughness peaks on the sample surface. Analogue to electric discharge machining (EDM), which has already been applied for machining insulating ceramics [16], this effect can be responsible for material removal. Owing to the minimal diameter of the plasma filament, space-resolved plasma polishing of complex-shaped work pieces made of Al_2O_3 could be realized by applying the presented plasma treatment method.

Table 1: Measured values for the surface roughnesses *Ra* and *RMS*, the surface energy γ and the polarity *P* of untreated and plasma-treated Al_2O_3 and the resulting percentual change

	Untreated Al_2O_3	Plasma-treated Al_2O_3	Change in %
Ra in nm	37.00	30.40	-17.84
RMS in nm	57.00	40.30	-29.30
γ in mJ/m²	42.02	52.03	+23.82
P	0.09	0.27	+200.00

The surface roughness has a strong influence on the wettability characteristics of Al_2O_3-based material surfaces. With surface smoothing, a reduction of the contact angle of test liquids and a corresponding increase in surface energy results [17]. This interrelationship was also observed for plasma-treated Al_2O_3 in the presented work. The disperse and polar fraction, the total amount of the surface energy γ and the associated polarity *P* before and after plasma treatment were determined according to the Owens-Wendt-Rabel-Kaelble (OWKR) method [18,19]. With the plasma treatment, both the surface energy γ and the polarity *P* of the investigated samples were significantly increased as shown in Table 1.

Besides the observed surface smoothing, plasma-induced surface cleaning can also effect an increase in surface energy by removing contaminations, which result from the sintering process, from the sample surface. The significant increase in polarity can be explained with the polar group rotation model. Here, a rotation of polar groups, which are embedded in the substrate, towards the surface results from the electric field of the plasma or related processes [20]. Further, plasma-induced melting and vitrification of residues of the smoothed roughness peaks can be involved in the observed increase in polarity [21].

(2) Laser-plasma ablation

In previous work, an increase in ablation rate of optical glasses [15] and aluminium [22] was shown when atmospheric pressure argon plasma is simultaneously introduced to the laser ablation process. Such a plasma-induced increase was also observed for Al_2O_3. Since a comparison of the particular ablation depth could not be performed owing to the inhomogeneous depth profile on the bottom of the ablated areas, minimum circumscribed circles (*MCC*) according to DIN EN ISO 1101 were used for describing and comparing the ablation efficiencies as shown for example for an applied laser energy of 95.9 mJ in Fig. 3.

In the case of pure laser ablation, the maximum ablated diameter $MCC_l \approx 295$ µm is obtained at approx. 20 – 30 laser pulses. In contrast, the measured MCC_{lp} for laser-plasma ablation increases linearly without approaching a saturation value after 40 applied laser pulses. As shown by the ratio of the detected minimum circumscribed circles for laser-plasma ablation and pure laser ablation in Fig. 4, the atmospheric pressure argon plasma does not provide a constant amount of additional energy for ablation.

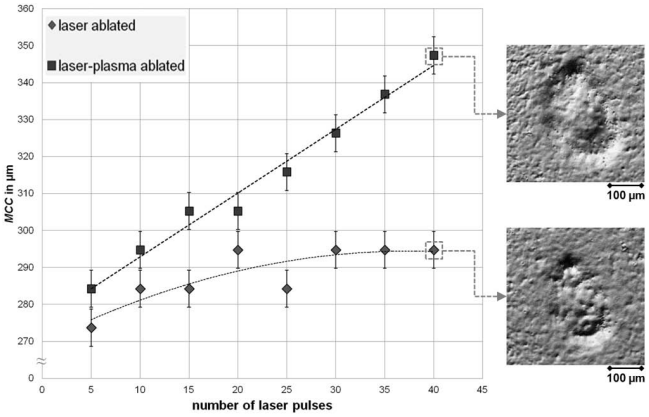

Fig. 3: Minimum circumscribed circles (*MCC*) of laser-ablated and laser-plasma-ablated Al_2O_3 surfaces vs. number of laser pulses.

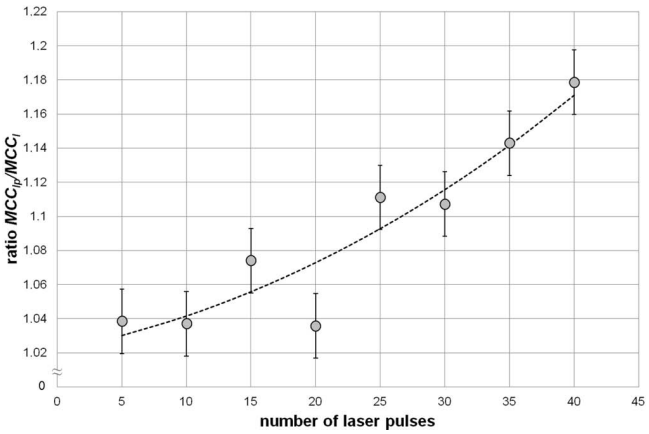

Fig. 4: Ratio of minimum circumscribed circles of laser-plasma-ablated and laser-ablated Al_2O_3.

Its influence on the ablation process increases when the number of laser pulses is increased. This can be explained by the fact that excited argon atoms and metastable argon species are generated and accumulated within the plasma volume between two laser pulses. Owing to radial diffusion and de-excitation at walls, these species are lost [23] with an according energy transfer. For the presented laser-plasma ablation setup, such walls are given by the sample itself and the resulting debris plume that is formed by each laser pulse, the surface of the debris plume being many orders of magnitude higher than the irradiated area on the sample surface. As a result, an additional amount of energy is deposited close to the sample surface.

Further, in the case of hybrid laser-plasma ablation, laser heating results in high temperatures in the range of approx. 5000 – 6000 K near to the sample surface. At such temperatures, argon plasmas have already been used to gain pure aluminium from aluminium oxide [24,25]. This process is described by an initial formation of monoxide,

$$Al_2O_3 \rightarrow 2AlO + O, \quad (1)$$

and a subsequent dissociation of *AlO* according to

$$AlO \rightarrow Al + O \quad (2)$$

This plasma-induced chemical reaction can also contribute to an increase in material removal during laser-plasma ablation.

Consideration of the laser-energy-dependent ablation results shows that the plasma-induced effect increases when the laser energy is reduced. For this purpose, the roundness form error according to the minimum zone circle (MZC) method (DIN EN ISO 1101) as well as the mean circle, i.e. the arithmetic mean diameter of both the *MCC* and the inner minimum circle, were analysed in addition to the *MCC*. Fig. 5 shows a comparison of the plasma influence on these parameters as a function of the laser energy. Here, the particular ratios (mean values for 20, 30 and 40 laser pulses) of laser-plasma ablation and pure laser ablation are shown.

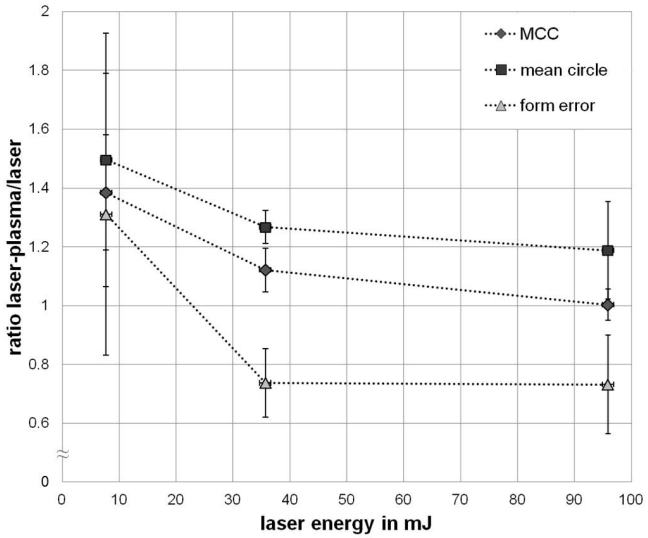

Fig. 5: Comparison of the plasma influence on the *MCC*, the mean circle and the form error vs. laser energy.

For this comparison, the measured values for ablation applying 5 – 10 pulses were not taken into account since in this case, no material removal was achieved by means of pure laser ablation at 7.7 and 35.7 mJ. This fact indicates a plasma-induced decrease in the laser ablation threshold, which is beneficial with regard to economic considerations. Further, production-relevant parameters are significantly improved for a number of different process settings by the assisting plasma. As an example, when ablation is performed applying ten laser pulses at 95.9 mJ, the form error is reduced by a factor of 1.8 whereas the mean circle diameter is increased by a factor of 1.4. This exemplifies the potential of introducing atmospheric pressure plasma to existing laser ablation techniques.

The strong influence of the assisting plasma in the case of laser-plasma ablation was also confirmed with spectroscopic measurements performed during laser ablation and laser-plasma ablation. Here, the exposure time was 500 ns. When the pure plasma beam was applied onto the sample surface, no spectral lines excepting characteristic argon peaks were detected. Nevertheless, as shown by the comparison of the roughness in section 3.1, a considerable material removal takes place during pure plasma treatment. However, this marginal amount of ablated material could not be measured with the used experimental setup for spectroscopy.

In the case of laser ablation, characteristic peaks of aluminium ions (Al II) were measured within the ablation plume. As shown by the comparison of the detected spectra for laser ablation, laser-plasma ablation and the difference spectrum of both spectra in Fig. 6, those peaks were significantly intensified when the plasma was applied simultaneously. In addition, atomic argon (Ar I) at 565.913 nm[26] of the used process gas was detected.

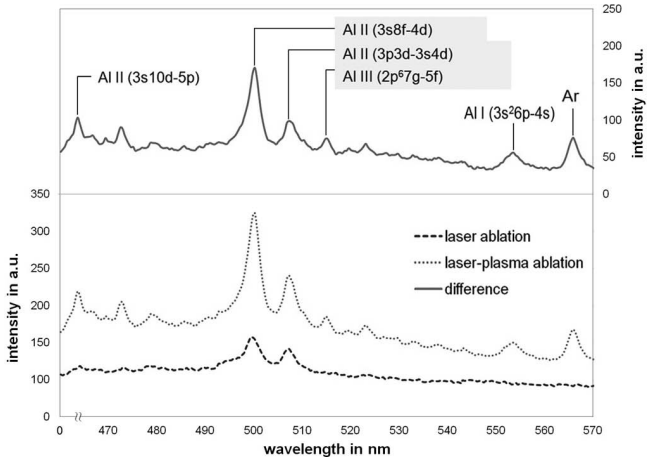

Fig. 6: Spectra of the ablation plume for laser ablation, laser-plasma ablation and the difference spectrum of both.

Besides such intensification, further spectral lines of atomic aluminium and different aluminium ions were observed during the hybrid ablation process as listed in Table 2.

Table 2: Al-peaks and corresponding transitions of Al-ions observed in the case of laser-plasma ablation of Al_2O_3.

Wavelength λ in nm	Transition	Ion
463.576	3s10d-5p	Al II [27]
500.097	3s8f-4d	Al II [28]
508.502	3p3d-3s4d	Al II [28]
515.101	$2p^6$7 g-5f	Al III [29]
555.706	$3s^2$6p-4s	Al I [30]

The spectroscopic measurement thus confirms an additional energy deposition into the sample surface and the debris plume as well as the corresponding increased amount of ablated material. Fig. 7 illustrates this plasma-induced effect.

Here, laser ablation and laser-plasma ablation was performed to drill holes into a sample bulk material. For this purpose, the laser was run for 60 s at a repetition rate of 10 Hz, resulting in a total number of 600 applied laser pulses.

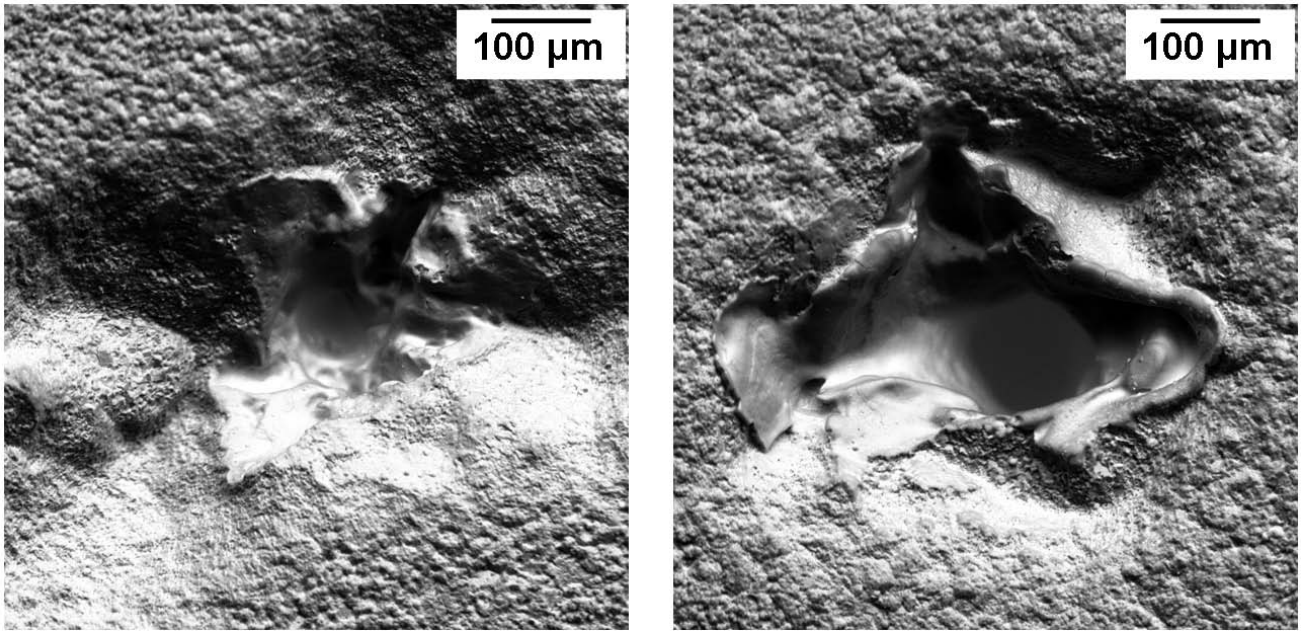

Fig. 7: Drilled holes in Al_2O_3, pure laser drilling (left) and laser-plasma drilling (right).

IV. Conclusions

Atmospheric pressure plasma treatment using argon as process gas allows a surface smoothing and an increase in both surface energy and polarity of aluminium oxide surfaces. As a result, the wettability of such surfaces is modified significantly. Concerning laser ablation of aluminium oxide, it was shown that the assisting plasma enables a reduction in the ablation threshold. Further, the ablation process was enhanced with improved contour accuracy and an increase in the amount of ablated material. These effects could be used for improving the machining properties, shortening process times and saving laser energy during micro-structuring of devices made of ceramic such as micro-electro-mechanical system components. For this purpose, further experiments to investigate the dependence of different process gases, the traverse speed, etc. on the ablation result need to be performed in order to parameterize the hybrid ablation process. However, it can be stated that combining atmospheric plasma treatment with a laser ablation process offers a variety of new advantageous effects based on the resulting synergies of the two techniques.

Acknowledgements

This work was supported by the European Regional Development Funds (EFRE) and the Workgroup Innovative Projects of Lower Saxony (AGiP) within the framework of the Lower Saxony Innovation Network for Plasma Technology (NIP), project funding reference number W2 – 80029388.

References

1 Lee, J.-M., Cho, I.-T., Lee, J.-H., Cheong, W.-S., Hwang, C.-S., Kwon, H.-I.: Comparative study of electrical instabilities in top-gate InGaZnO thin film transistors with Al_2O_3 and Al_2O_3/SiN_x gate dielectrics, *Appl. Phys. Lett.*, **94**, 222112, (2009).

2 Khan, J.: A lapping and polishing process to achieve high quality alumina surfaces for applications in device fabrication, *Thin Solid Films*, **220**, 222 – 226, (1992).

3 Kawakami, K., Suda, M., Aihra, M., Fukuoka, H., Hagiwara, Y., Tekeshita, K.: Electrical detection of end point in polishing process of thin film heads, *J. Appl. Phys.*, **61**, 4163 – 4166, (1987).

4 Tönshoff, H.K., Emmelmann, C.: Laser cutting of advanced ceramics, *CIRP Ann.*, **38**, 219 – 222, (1989).

5 Perrie, W., Rushton, A., Gill, M., Fox, P., O'Neill, W.: Femtosecond laser micro-structuring of alumina ceramic, *Appl. Surf. Sci.*, **248**, 213 – 217, (2005).

6 Kim, S.H., Sohn, I.-B., Jeong, S.: Ablation characteristics of aluminum oxide and nitride ceramics during femtosecond laser micromachining, *Appl. Surf. Sci.*, **255**, 9717 – 9720, (2009).

7 Kim, S.H., Balasubramani, T., Sohn, I.-B., Noh, Y.-C., Lee, J., Lee, J.B., Jeong, S: Precision microfabrication of AlN and Al_2O_3 ceramics by femtosecond laser ablation. In: Proceedings of SPIE 6879, 2008.

8 Ho, C.Y., Lu, J.K.: A closed form solution for laser drilling of silicon nitride and alumina ceramics, *J. Mater. Process. Tech.*, **140**, 260 – 263, (2003).

9 Klimentov, S.M., Garnov, S.V., Kononenko, T.V., Konov, V.I., Pivovarov, P.A., Dausinger, F.: High rate deep channel ablative formation by picosecond-nanosecond combined laser pulses, *Appl. Phys. A*, **69** [Suppl.], S633 – S636, (1999).

10 Kononenko, T.V., Garnov, S.V., Klimentov, S.M., Konov, V.I., Loubnin, E.N., Dausinger, F., Raiber, A., Taut C.: Laser ablation of metals and ceramics in picosecond-nanosecond pulse width in the presence of different ambient atmospheres, *Appl. Surf. Sci.*, **109/110**, 48 – 51, (1997).

11 Geiger, M., Becker, W., Rebhan, T., Hutfless, J., Lutz, N.: Increase of efficiency for the XeCl excimer laser ablation of ceramics, *Appl. Surf. Sci.*, **96 – 98**, 309 – 315, (1996).

12 Viöl, W., Wieneke, S., Damm, R., Brückner, S.: Hollow funnel shaped plasma generator, WO 2011095245 (A1), 2011.

13 Brückner, S., Rösner, S., Gerhard, C., Wieneke, S., Viöl, W.: Plasma-based ionisation spectroscopy for material analysis, *Mater. Test.*, **53**, 639 – 642, (2011).

14 Oliveira, V., Orlianges, J.C., Catherinot, A., Conde, O., Vilar, R.: Laser ablation of Al_2O_3-TiC: a spectroscopic investigation, *Appl. Surf. Sci.*, **186**, 309 – 314, (2002).

15 Gerhard, C., Roux, S., Brückner, S., Wieneke, S., Viöl, W.: Low-temperature atmospheric pressure argon plasma treatment and hybrid laser-plasma ablation of barite crown and heavy flint glass, *Appl. Optics*, **51**, 3847 – 3852, (2012).

16 Mohri, N., Fukuzawa, Y., Tani, T., Saito, N., Furutani, K.: Assisting electrode method for machining insulating ceramics, *CIRP Ann.*, **45**, 201 – 204, (1996).

17 Lawrence, J., Li, L.: Wettability characteristics of an Al_2O_3/SiO_2-based ceramic modified with CO_2, Nd:YAG, excimer and high-power diode lasers, *J. Phys. D.*, **32**, 1075 – 1082, (1999).

18 Kaelble, D.H.: Peel adhesion: influence of surface energies and adhesive rheology, *J. Adhes. Sci. Technol.*, **1**, 102 – 123, (1969).

19 Owens, D.K., Wendt, R.C.: Estimation of the surface free energy of polymers, *J. Appl. Polym. Sci.*, **13**, 1741 – 1747, (1969).

20 Roth, J.R.: Industrial Plasma Engineering Vol. 2. 1st edition. Institute of Physics Publishing, London, 2001.

21 Agathopoulos, S., Nikolopoulos, P.: Wettability and interfacial interactions in bioceramic-body-liquid systems, *J. Biomed. Mater. Res.*, **29**, 421 – 429, (1995).

22 Gerhard, C., Roux, S., Brückner, S., Wieneke, S., Viöl, W.: Atmospheric pressure argon plasma-assisted enhancement of laser ablation of aluminum, *Appl. Phys. A*, **108**, 107 – 112, (2012).

23 Bogaerts, A., Gijbels, R.: Comparison of argon and neon as discharge gases in a direct-current glow discharge – a mathematical simulation, *Spectrochim. Acta B*, **52**, 553 – 565, (1997).

24 Rains, R.K., Kadlec, R.H.: The reduction of Al_2O_3 to aluminum in a plasma, *Metall. Mater. Trans. B*, **1**, 1501 – 1506, (1970).

25 Fridman, A.: Plasma Chemistry. 1st edition. Cambridge University Press, Cambridge, 2008.

26 Bues, I., Haag, T., Richter, J.: Transition probabilities, broadening and shifting of neutral argon lines. In: Institut für Experimentalphysik der Universität Kiel Technical Report. Christian-Albrechts-Universität, Kiel, Germany, 1969.

27 Kaufman, V., Hagan, L.: Spectrum and energy levels of single ionized aluminum (Al II), *J. Opt. Soc. Am.*, **69**, 232 – 239, (1979).

28 Sawyer, R.A., Paschen, F.: The first spark spectrum of the aluminium Al II, (in German), *Ann. Phys.*, **389**, 1 – 19, (1927).

29 Isberg, B.: The spectrum of doubly ionized aluminium, Al III, *Ark. Fys.*, **35**, 551 – 562, (1968).

30 Eriksson, K.B.S., Isberg, H.B.S.: The spectrum of atomic aluminium, Al I, *Ark. Fys.*, **23**, 527 – 542, (1963).